LANGMUIR

Article

Triazole/triazine-functionalized mesoporous silica as a hybrid material support for palladium nanocatalyst

ALI SAAD, Christian Vard, Manef Abderrabba, and Mohamed Mehdi Chehimi

Langmuir, **Just Accepted Manuscript** • Publication Date (Web): 21 Jun 2017

ACS Publications

Langmuir is published by the American Chemical Society. 1155 Sixteenth Street N.W., Washington, DC 20036

Triazole/triazine-functionalized mesoporous silica as a hybrid material support for palladium nanocatalyst

Ali Saad [a, b *], *Christian Vard* [c], *Manef Abderrabba* [a, *] *Mohamed M. Chehimi* [c, *]

a) *Laboratory of Materials, Molecules and Applications, IPEST, University of Carthage, Sidi Bou Said road, B.P. 51 2070, La Marsa, Tunisia.*
b) *Faculté des Sciences de Tunis, Université El Manar, PO Box 248, El Manar II, 2092, Tunis, Tunisia.*
c) *Université Paris Est, ICMPE (UMR 7182), CNRS, UPEC, 2-8 rue Henri Dunant, 94320 Thiais, France.*

Abstract

Noble and precious metal catalysts are sought for their remarkable efficiency in catalyzing numerous reactions in heterogeneous phase. However, they are costly and request the development of high surface area supports that favor their strong immobilization, dispersion and stability. Towards this end, mesoporous silica-based materials can be regarded as unique supports for nanometric-sized noble metal catalysts provided they are functionalized with appropriate ligands. In this work, mesoporous silica SBA-15 was prepared and modified with 3-azidopropyltriethoxysilane then clicked with alkyne derivatives of 1,3,5-triazines complex ligand. The resulting hybrid material contains triazole and triazine moieties covalently bound to the mesoporous silica network. The triazole/triazine mini-dendron was immobilized through 1,3-dipolar cycloaddition click reaction which was monitored using Fourier transform infrared spectroscopy (FTIR), X-ray photoelectron spectroscopy (XPS). The heterocyclic ligand-functionalized SBA-15 material served as hybrid reactive platform for the in situ deposition of palladium nanoparticles whose size is 3.154 ±0.49 nm as assessed by XRD and confirmed by TEM. The catalytic performances of the final palladium-decorated hybrid triazole/triazine-functionalized SBA-15 support were evaluated in the model reduction of p-nitrophenol (p-NP) into p-aminophenol (p-AP) by catalytic hydrogenation and stoichiometric reduction. Excellent catalytic performances were achieved, with reduction rate constant (K_{app}) of 16.8×10^{-3} s^{-1} for this model reaction. Moreover, the hybrid catalyst can be produced in high yield and recycled.

Keywords: mesoporous silica, 3-azidopropyltriethoxysilane, nitrogen heterocycles, click chemistry, Pd nanocatalyst.

Corresponding authors:
Ali Saad: ali.saad8803@gmail.com
Manef Abderrabba: abderrabbamanef@gmail.com
Mohamed M. Chehimi: chehimi@icmpe.cnrs.fr

1 Introduction

Palladium nanoparticles (PdNPs) have received considerable attention due to remarkable catalytic performances in the reduction of nitro compounds.[1,2,3] They were also recognized to be efficient catalysts of various organic chemical reactions in the chemical and pharmaceutical industries, including Suzuki–Miyaura coupling,[4,5] O- and N-arylations,[6] and oxidation of alcohols.[7] Interestingly, PdNPs can be even be produced as mesoporous structures with unprecedented electrocatalytic performances.[8,9,10] However, it is difficult to separate and thus to recover noble metal catalysts from the reaction mixture, with a result of adverse environmental pollution, which limits their applications. To address this concern and in order to facilitate the catalyst recovery, PdNPs are commonly dispersed onto solid matrices to prepare heterogeneous palladium catalysts. Indeed, in order to limit agglomeration of Pd nanoparticles, it is possible to immobilize them on various solid supports such as amorphous silica,[11] titania,[12]carbon,[13] core–shell magnetic fibers[14] and hexagonally ordered mesoporous silica.[15,16] Particularly, mesoporous silica offers great advantages due to its outstanding features such as high surface area, regular tunable and accessible pores and control over their sizes, high thermal stability, and mechanical properties.[17,18,19,20] One can take advantage of the nature of mesoporous silica pore structure to functionalize it with alkoxysilyl compounds in order to facilitate the incorporation of metal complexes in the said pores.[21,22]

An attractive method that allows for fine-tuning of catalytic material at the molecular level consists in the use of organic molecules for covalent functionalization. Another commonly followed route is the functionalization of mesoporous silica via addition reactions, namely cycloaddition, nucleophilic and free-radical additions, and reductive alkylation onto/inside the silica pores in order to design hybrid materials.[23] Among the most investigated click reactions (Huisgen 1,3-cycloaddition, Diels-Alder, thiol-yne, thiol-ene, Michael addition), Huisgen reaction has raised much interest owing to its simplicity and efficiency either in bulk solutions or in suspensions where it is employed to functionalize or bridge compounds, and plays a very important role in the design of novel hybrid materials.[24] Huisgen reaction is actually one of the most efficient routes for binding appropriately functionalized molecules to solid supports through triazole linkages. Therefore, azido-functionalized SBA-15 materials have been widely employed to covalently attach various moieties to the inorganic support. For example, mesoporous silica-based hybrid materials were designed and evaluated in biosensing applications,[25] removal of antibiotics,[26] immobilization of enzymes[27] and as catalyst supports,[28] to name but a few.

It is well known that N-2 and N-3 nitrogen atoms present in the triazole ring are good H-bond acceptors owing to the 1,2,3-triazole large dipole moment.[29] Moreover, triazole groups are excellent nitrogen-donor ligands and thus are ideal for coordinating a variety of transition metals.[30, 31] As far as triazine derivatives are concerned, they belong to the compounds with nitrogen–carbon double bonds and which exhibit excellent ability to immobilize proteins[32] and catalysts[31] on the underlying materials surfaces. One can take advantage of the chemical and electronic structure of triazine to implement this functional group in the inorganic/organic hybrid systems in order to enhance the coordination of metal ions[33] and therefore to design a support for anchoring metal NPs evenly dispersed on the active sites.[34]

Whilst triazine and triazole were used separately to functionalize mesoporous silicas for the in situ deposition of metallic nanocatalysts, we have reasoned that we can take advantage of their remarkable and synergetic properties in view of making one single dendron-like structure attached to silicas in view of immobilizing the said metallic nanocatalysts. With this objective in sight, we relied on the efficiency of click chemistry to prepare a clickable dendron-like nitrogen heterocyclic structure to react with azido-functionalized mesoporous SBA-15 and end up with a unique organic/inorganic hybrid platform for dispersing and immobilizing nanocatalysts. To the very best of our knowledge this strategy has not been described previously; this is what has motivated us to construct the unique hybrid materials for the attachment of metallic nanocatalysts.

Herein, we have prepared palladium NPs supported on 1,2,3-triazoles from alkyne derivatives of 1,3,5-triazine complexes, designed via ‘‘click’’ chemistry. The rationale for using a high surface area support (mesoporous silica) is to achieve excellent dispersion of the nanocatalyst and to enhance its catalytic activity. Metal complex speciation and catalytic reaction were shown to be influenced by surface loading. In addition, it is important to chemically tailor an environment within the support to achieve metal affinity and ligand stability.[35,36] The Pd-catalyzed reduction of 4-nitrophenol into aminophenol using $NaBH_4$ as reducing agent was performed in order to assess the catalytic performances of the hybrid silica-immobilized noble metal nanocatalyst.

The synthesis of 1,2,3-triazoles from alkyne derivatives of 1,3,5-triazines was obtained by 1,3-dipolar cycloaddition reactions between organic azides and terminal alkynes of trispropargylmelamine, using a three-step methodology (Figure 1): (i) a clickable group (N_3−) was introduced onto mesoporous silica by covalently grafting the azide using

azidopropylsilane ; (ii) synthesis of trispropargylmelamine; and (iii) the click chemistry reaction inside the mesoporous silica formed organic compounds triazole-triazine complexes grafted into the pores. The nitrogen-rich triazole/triazine group is expected to act as bidendate or even multidentate ligand towards Pd(II) ions. This chelation mechanism leads to the dispersion and stabilization of the Pd NPs on the hybrid mesoporous support.

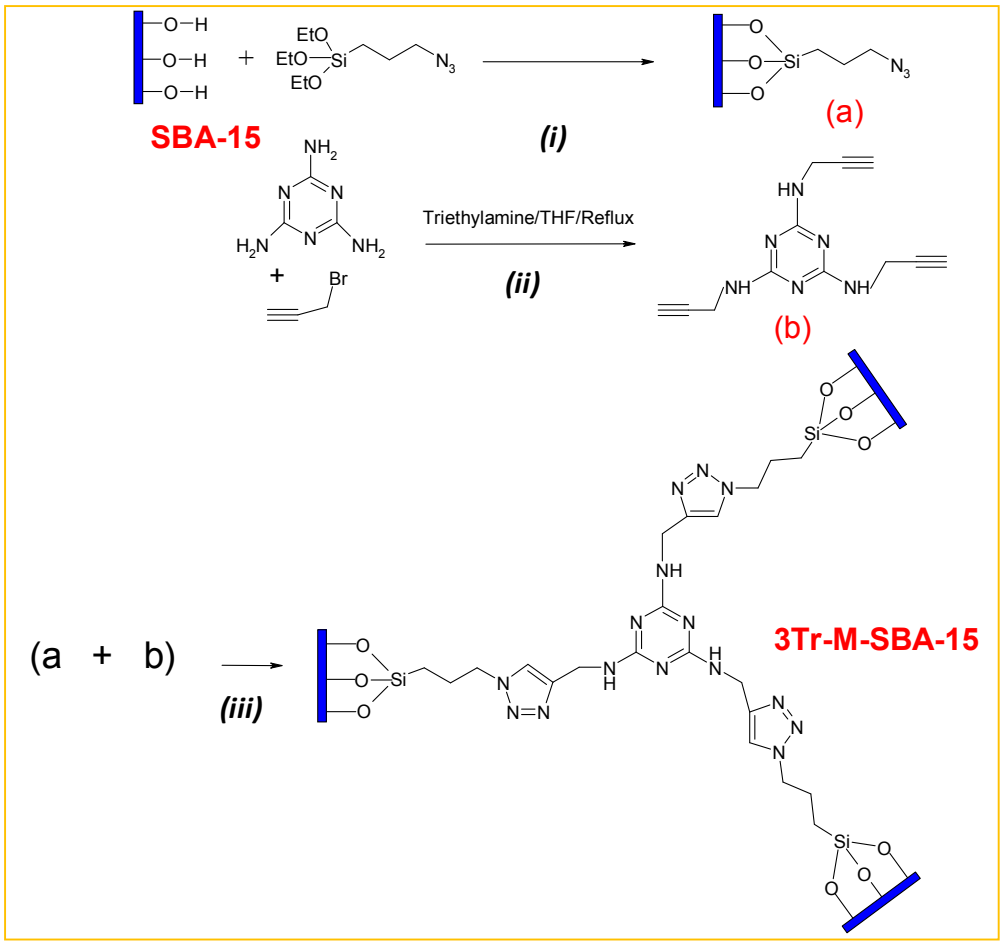

Figure 1. Schematic representation of the preparation 1,2,3-triazoles from alkyne derivatives of 1,3,5-triazines complex supported mesoporous silica palladium complex.

2 Experimental

2.1 Materials

Poly(ethyleneoxide)-b-poly(propyleneoxide)-b-poly(ethylene-oxide) [EO20PO70EO20, Pluronic P123, M_w = 5800], tetraethylorthosilicate (TEOS, 98%), 3-

chloropropyltriethoxysilane, triethylamine, tetrahexylammonium bromide, sodium ascorbate, sodium azide (NaN_3), 1,3,5-triamino-triazine (melamine), propargyl bromide (80%), copper (II) sulfate pentahydrate ($CuSO_4 \cdot 5H_2O$), toluene, pentane, acetonitrile, propan-2-ol, tetrahydrofurane (THF), HCl and ethanol (Aldrich-Sigma products) were of high purity grade and used as received. Water was deionized using the Milli-Q system of Millipore.

2.2. Synthesis of SBA-15 mesoporous silica

The mesoporous SBA-15 was synthesized following the procedure described by Zhao et al.[37] First, 3g of nonionic triblock copolymer Pluronic P123 was dissolved in16.5 ml of HCl (12 M) and 112 ml of water. The solution was vigorously stirred for 3 h at 40 °C. Second, after complete dissolution of Pluronic P123, 7.427 g of TEOS was rapidly added to the acidic solution under continuous stirring. A synthesized gel was obtained after resting for 2 h at 40 °C the mixture was transferred to an oven for further condensation at 90 °C under static conditions for 24 h. The precipitate obtained after filtration was washed and dried. Finally, the template removal from as synthesized SBA-15 was removed by calcination (550 °C, 8 h).

2.3. Preparation of Pd(II)/1,2,3-triazole from alkyne derivatives of 1,3,5-triazine complex supported mesoporous silica

2.3.1 Synthesis of N_3-SBA-15.

The 3-azidopropyltriethoxysilane was prepared according to the literature.[23,27] To a solution of tetrahexylammonium bromide (0.86 g, 2 mmol) and sodium azide (1.08 g, 16.6 mmol) in dry acetonitrile (50 mL) was added 3-chloropropyltriethoxysilane (2 g, 8.3 mmol). The heterogeneous mixture was then heated to 82 °C under an inert atmosphere for 18 h. After completion of the reaction, the solvent was removed under reduced pressure, and the crude mixture was diluted with pentane. The suspension was filtered through celite and the solvent was removed by vacuum distillation. The 3-azidopropyltriethoxysilane (AzPTES) was obtained as a colorless liquid. ^{1}H NMR ($CDCl_3$): δ (ppm) = 3.75 (q, 6 H; CH_3CH_2O), 3.20 (t, 2H; CH_2N_3), 1.64 (m, 2H; $SiCH_2CH_2$), 1.16 (t, 9H, CH_3CH_2O), 0.61 (m, 2H; $SiCH_2$).

To a suspension of 1 g of SBA-15 in 50 mL of toluene, 2 mL AzPTES were added, and the mixture was stirred for 24 h at 80 °C under nitrogen atmosphere. After the completion of the reaction, the products were cooled, filtered and washed with toluene until it became free from AzPTES. The sample was then dried at 80 °C for 8 h.

2.3.3. Synthesis of trispropargyl melamine "3Tr-M"

0.87 g (6.9 mmol) of 1,3,5-triamino-triazine was added to a mixture of 3.65 g of propargyl bromide (80%) and triethylamine (0.68 g, 6.9 mmol) in THF (120 mL). The solution was then heated to 80 °C for 24 h and filtered. The filtrate was dried under vacuum. Finally the product was isolated as a white powder and was then dried at 70 °C.

2.3.3. Synthesis of 3Tr-M-SBA-15

3Tr-M-SBA-15 was obtained by 1,3-dipolar cycloaddition reactions as follows: the N_3-SBA-15 (1.22g), CuSO4 (0.43, 0.1M), and sodium ascorbate solution (0.77g, 0.1M) was added to a solution of trispropargyl melamine (0.15, 1M) in 50% aqueous propan-2-ol (20 ml) under stirring for 24 h at 25 °C. The resulting product 3Tr-M-SBA-15 was filtered and washed thoroughly with ethanol and acetone and dried under vacuum for 24 hours.

2.3.4. In-situ synthesis of palladium nanoparticles

At first, palladium catalyst was prepared according to Chergui et al. [38] Chelatant nanosupports 3Tr-M-SBA-15 (50 mg) were ultrasonically dispersed in 10 mL of NaOH solution (1 M), and then 10 mL of an aqueous solution of $PdCl_2$ (10^{-2} M) was added. After stirring for1h, subsequent reduction of the metal was performed by addition a fresh aqueous solution of $NaBH_4$ (0.1M), to the mixture. The solution was stirred for 1 h at room temperature. The resulting palladium nanoparticle-decorated mesoporous silica were filtered, then washed several times with water, and dried under vacuum.

2.4. Catalytic reduction of 4-nitrophenol

Typically, in a standard quartz cuvette, 4-nitrophenol (30 µL, 7.4 mM), $NaBH_4$ (30 µL, 0.82 M), and deionized water (2 mL) were added. After adding Pd/3Tr-M-SBA-15 17 µL catalyst (1.75 g/L), the mixture was vigorously stirred using a small glass stirring rod. As the reaction progressed, the bright yellow color of the solution gradually faded. UV−vis spectra were taken after set periods of time. After the catalytic reaction was completed, the catalyst was collected and washed with ethanol prior to reuse for a next catalytic test.

2.5. Characterization

A K Alpha (Thermo) machine equipped with a monochromatic, 400 µm-sized Al K X-ray source was used for X-ray photoelectron spectroscopy (XPS) measurements. The pass energy was set to 200 and 50 eV for the survey and the narrow regions, respectively. The C-C/C-H

C1s component was set at 285 eV to calibrate the spectra. The composition was assessed using the sensitivity factors provided by the manufacturer.

Nitrogen adsorption and desorption studies were carried out at 100 °C and 0.1 MPa for 12 h before measurements using a autosorb IQ, Quantachrome. The specific surface (S_{BET}) values were obtained using the Brunauer-Emmett-Teller (BET) method[39] whereas the mesopore size was assessed using the Barrett-Joyner-Halenda (BJH) method[40] from the desorption branch of the isotherm.

The thermal and decomposition characteristics of the materials were determined by thermal gravimetric analyses, were performed using a SETSYS evolution 16 apparatus from SETARAM, in the temperature range of 10-800 °C with a heating rate of 10C/min under a flow of air at (55 cm^3 (STP)/min) with a heating rate of 10 °C min^{-1}.

Fourier transform infrared (FTIR) spectra were recorded using an EQUINOX 55 (Bruker) Spectrometer ranging from 4000 to 400 cm^{-1}. Spectra were accumulated 64 times at 4 cm^{-1} resolution and processed using OPUS/IR software.

Transmission electron micrographs were obtained on a (TEM-Tecnai F20 with a Field Emission Gun 200 kV, punctual resolution 0.24 nm and Energy Filtering GIF). Samples were prepared by dispersing in ethanol using an ultrasonic bath. Few drops from these suspensions were then gently deposited onto a carbon-covered copper grid and then ethanol was evaporated.

The ^{1}H, and ^{13}C NMR spectra were obtained with a Bruker AVANCE 300 wide bore spectrometer using deuterated chloroform as the solvent and internal standard. The chemical shifts are reported in parts per million (ppm). The ^{13}C CP MAS NMR spectra were recorded on a Bruker AVANCE 400 wide bore spectrometer with a 12-kHz MAS spinning rate (the typical contact time was 3ms, and Typically 10000 to 25000 scans with a recycle delay of 3s were collected depending on the sensitivity of the sample.

3. Results and discussion

3.1. Physicochemical properties of materials

3.1.1. FT-IR spectroscopy analysis.

The FT-IR spectra before and after inclusion of propargylamine are presented in Figure 2a. The spectrum for pure 1,3,5-triamino-triazine exhibits the characteristic absorption bands in the 478–1662 cm^{-1} range *i.e.* 1624, 1532, 1428, 808 and 584 cm^{-1} bands can be assigned to the aromatic stretching modes in triazine ring, C=N (imine stretching) in-plane deformation, C-N stretching and C–H outer-bending vibrations, respectively. These characteristic bands of the triazine ring also appear after reaction with propargyl bromide. Also as can be seen appearance of the new adsorption peaks at 2109, 2923, 2961, 3128 and 3244 cm^{-1} are due to (C-C≡CH) stretch, ν_{sy} CH in -CH_2 – group), ν_{as} CH (in -CH_2 – group), (N-H secondary amine) and the alkyne C-H vibrations. All these bands confirmed the successful obtaining the desired compound. Figure 2b shows spectra of SBA-15 based materials. The (3-azidopropyl) triethoxysilane grafted mesoporous silica yields a new peak observed at 2110 cm^{-1} which is a characteristic stretching vibration of organic azides.[26] This band confirms the effective incorporation of the azido functional group to the materials. The associated Si-O-Si bands are observed at 1274, 1050, 910, 797, and 448 cm^{-1}.[27] After the click reaction the typical band for the azido group was no longer present, indicating that the click reaction proceeded to completion. Upon clicking, a new band at 1610, 1470 and 1402 can be assigned to the aromatic stretching modes in triazine and triazole rings.[35, 41]

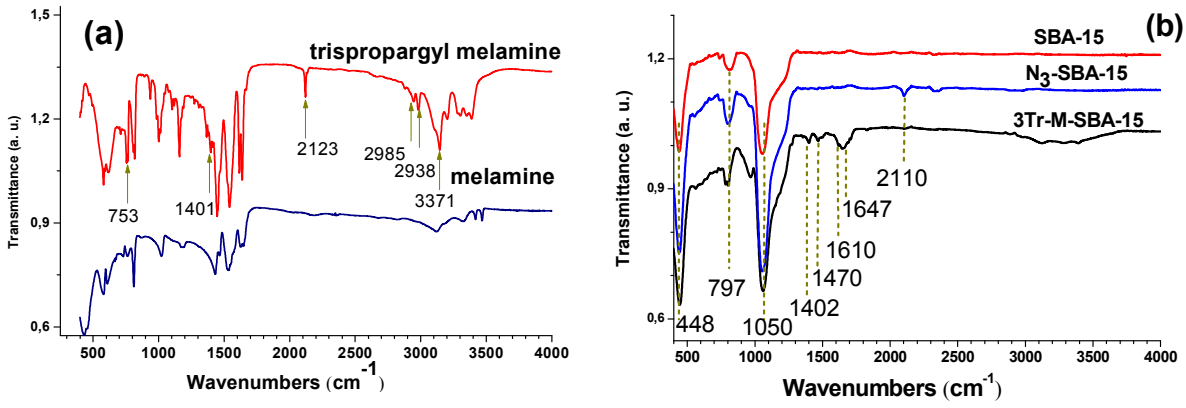

Figure 2. FTIR spectra of: (a) 1,3,5-triamino-triazine (melamine) before and after modification with propargyl bromide , (b) SBA-15, N_3-SBA-15 and 3Tr-M-SBA-15.

To confirm FT-IR studies we have employed solid state ^{13}C cross-polarized magic angle spinning (CP-MAS) NMR. N_3-SBA-15 and 3-Tr-M-SBA-15 spectra are displayed in Figure S1 (see Supporting Information). For the N_3-SBA-15 (Figure S1a), three peaks at δ= 9.4, 22.5 and 54 ppm are ascribed to the C signals of azidopropyl. One can also note additional peaks assigned to residual P123 template (71 and 17 ppm) and to EtO groups (59 and 17 ppm).[28] After azide-alkyne 1,3-dipolar cycloaddition (CuAAC) of N_3–SBA-15, along with all three peaks of propyl attached SBA-15, extra peaks are clearly visible at δ= 102, 125.5 and 132.9 ppm, which corresponds to the triazole-triazine group attached to the surface (Figure S1b).

3.1.2. Nitrogen adsorption–desorption isotherms.

The surface area, diameter and pore volume of SBA-15, N_3-SBA-15 and 3Tr-M-SBA-15 samples were assessed by nitrogen adsorption/desorption isotherms (Figure 3). The textural properties are gathered in Table 1. For all materials, it can be observed that, as defined by Brunauer et al.,[42] the sorption resulted in a typical type IV isotherm hysteresis loop at high relative pressure values (P/P_0 = 0.65). This behaviour is characteristic of materials possessing regular cylindrical mesopores with a narrow pore size distribution.[2]

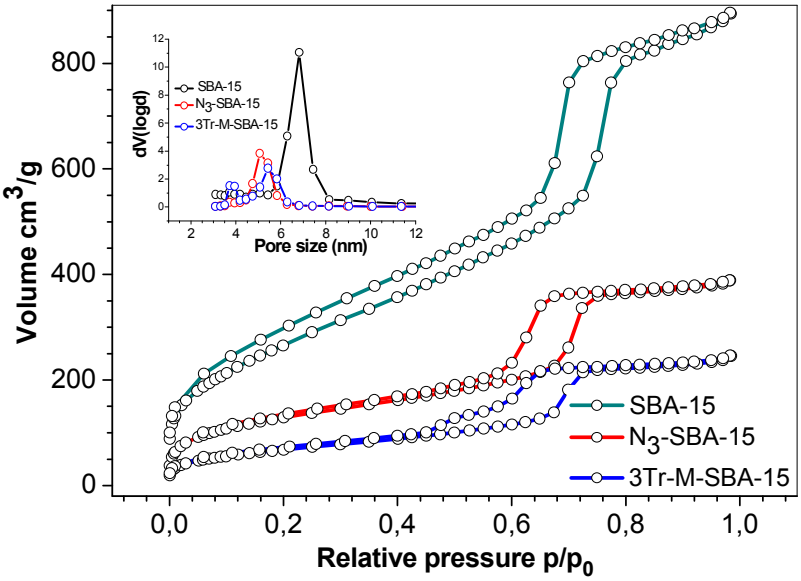

Figure 3. Nitrogen adsorption/desorption isotherms of (a) SBA-15, (b) N_3-SBA-15, (c) 3Tr-M-SBA-15.

The specific surface area, total pore volume, and pore size decreased with the increase of azide content as shown in Table 1. The multiple points BET surface areas of SBA-15, N_3-SBA-15 and 3Tr-M-SBA-15 were 734, 375 and 289 m^2/g, respectively. The pore size distribution, determined for pristine and modified SBA-15 samples by the BJH method, is also shown in Figure 3. The pore diameter (D_{BJH}) distributions of SBA-15, N_3-SBA-15 and 3Tr-M-SBA-15 are centered at ~ 6.8, 5.8 and 5.4 nm, respectively. However, the incorporation of organic groups to the mesoporous silica resulted in a decrease in pore volume compared to pristine SBA-15 (Table 1). This significant decrease in the porosity, surface area and total pore volume of the functionalized materials is due to the partial blocking of the pores by grafting of organic groups on the inner walls of SBA-15. [43]

Table 1. Specific surface areas, mean pore diameters and porous volumes for SBA-15 and ligand-modified SBA-15.

Materials	S_{BET} (m^2g^{-1})	D_p^{BJH} (nm)[a]	V_p (cm^3g^{-1})[b]
SBA-15	733	6.81	1.15
N_3-SBA-15	375	5.83	0.529
3Tr-M-SBA-15	289	5.43	0.374

[a] Mean pore diameter determined using the BJH method
[b] Total pore volume determined at $P/P^0 = 0.97$

3.1.3. XPS analysis

Figure 4 displays high-resolution C 1s and N 1s spectra of 3Tr-M-SBA-15 and its precursor N_3-SBA-15. For the latter, C1s is fitted with three components centered at 285, 286.7 and 288.7 eV, which are attributed to C-C/C-H, C-N and O-C=O, respectively (Figure 4a). The high binding energy component noted at 288.7 eV can be assigned to O-C=O from SBA-15. This feature is most of the time detected at the surface of the high energy materials such as metals, metal oxides and ceramics.[44] As far as the N 1s region is concerned, the spectrum is fitted with three components assigned to N-H/N-C (399-400 eV), N^-/N-C (~401 eV), and N^+ (~404.5 eV), respectively (Figure 4b). The N^+ atom is the central nitrogen atom in the azido group which co-exists in the following mesomeric forms: $-N=N^+=N^- \leftrightarrow -N^--N^+\equiv N$.[45] The main peak centred at ~401 is due to the two other nitrogen atoms which can be negatively charged. The first peak at 399-400 eV is assigned to N-H/N-C bonds. We would like to insist at this stage on the fact that azido groups are known to undergo X-ray photodegradation during XPS

analysis as we[24] and others[46] have demonstrated previously. As far as we are concerned we have given guidelines for analyzing material surface-bound azido groups. We have strictly followed the procedures in order to be able to check by XPS the presence of surface bound $-N_3$ prior to any significant X-ray induced photodegradation. After reaction with trispropargyl melamine, for 3Tr-M-SBA-15, the C=N/CN peak component is significantly higher (Figure 4c), suggesting that more N species have been incorporated into the skeleton of the support which is in the line with the surface elemental composition reported in Table S1.

The azide is transformed into triazole and the N^+ peak component has vanished indicating complete reaction, a result that supports the FTIR findings. The N=N atoms have a single component centred at 400.2 eV and the sp^3 nitrogen atom has a peak centred at 402 eV. The N1s region has additional component centred at 398.6 assigned to N=C (Figure 4d).

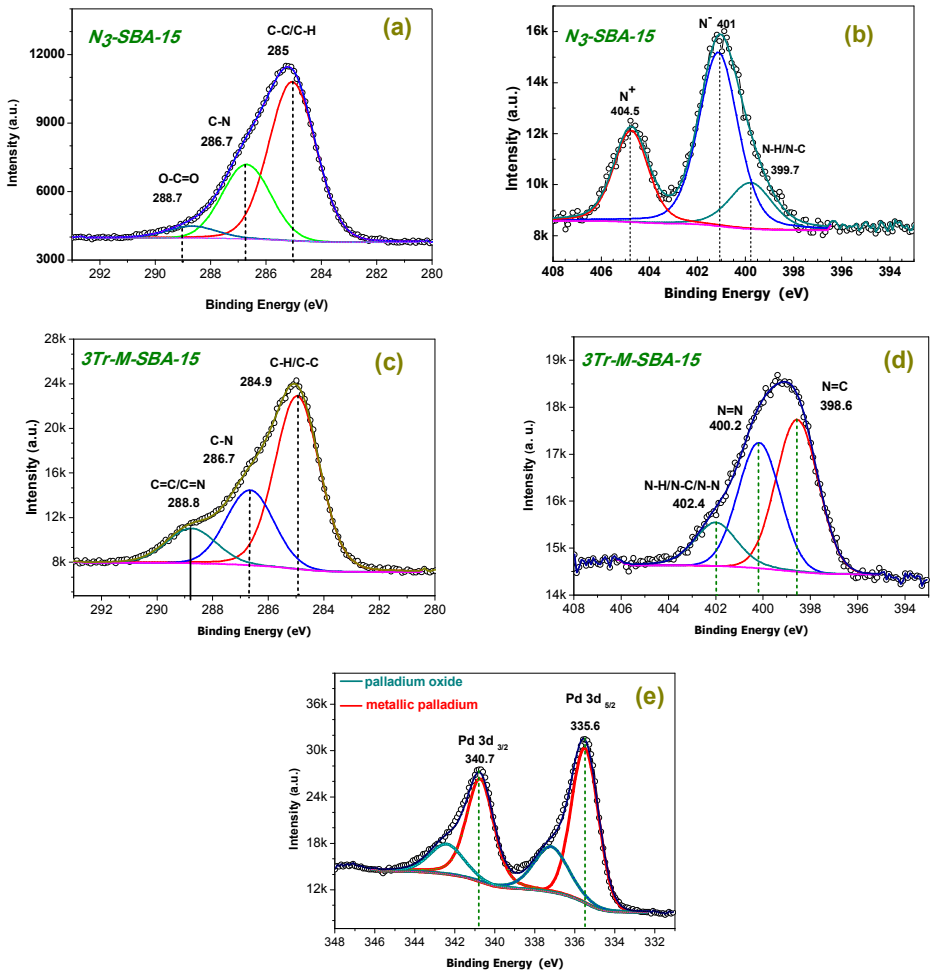

Figure 4. (a) C 1s , (b) N1s XPS spectra of the N_3-SBA-15 before , (c) C 1s , (d) N1s after click reaction with trispropargylmelamine and (e) Pd_{3d} after immobilization of palladium nanoparticles.

The electronic state of metallic palladium particles in the catalyst was further analyzed by the XPS spectrum. The result (Figure. 4e) demonstrated that the Pd $3d_{5/2}$ and $3d_{3/2}$ doublet binding energy positions are observed at 335.6 and 340.7 eV, which is consistent with the range of values compiled by Powell and co-workers [47] for palladium in the metallic state. Palladium is also detected in the oxidation state (doublet pair at 337.2 and 342.4 eV) due to Pd-O bond formation upon air exposure of the hybrid catalyst.

Table S1 reports the surface chemical composition of unmodified, azido-silanized and palladium immobilized grafted mesoporous silicas Pd(0)/3Tr-M-SBA-15. The N/Si atomic ratio is equal to ~0.09 after azido-silanization but increases to ~0.167 upon click chemistry grafting. Indeed, the mesoporous silica gets wrapped by the trispropargyl melamine which brings nitrogen atoms in melamine groups, hence the increase in the N/Si ratio. Incorporation of nitrogen-containing groups alters the surface composition and induces surface hydrophilic character which favors the dispersion in water and other polar solvents. The high extent of nitrogen atoms brought by the ligand facilitates the complexation of the Pd^{2+} ions and their tight immobilization onto the support. As previously demonstrated, pyridinic and quaternized N species facilitate the coordination of metal ions as well as the attachment of metal NPs.[35,48,49,50]

The XPS surface analysis of all materials permitted to track the subtle changes of the composition following azido-silanization and click chemistry grafting of trispropargyl melamine.

3.1.4. Thermal analysis

Thermal degradation of pristine and modified SBA-15 samples was studied using TGA by heating the samples from room temperature to 800 °C under a nitrogen atmosphere, at a rate of 10 °C min^{-1}. Thermogravimetric (TG) analyses were carried out to confirm the effective modification of silica with the functional groups resulting from silanization and subsequent click reaction. As shown in Figure 5 the first weight loss below 170 °C is ascribed to the volatilization of water adsorbed on all samples. A second significant weight loss of 12.7 and 23.4% can be observed between170 and 500 °C for N_3-SBA-15 and 3Tr-M-SBA-15. This weight loss is attributed to the decomposition of both the organic groups and the bridging

ethylene groups, respectively. Similar results were reported previously for other "click"-functionalized solid periodic mesoporous organosilica supports.[35, 51] The weight loss difference between azidopropyl functionalized mesoporous silica and triazole-triazine groups attached to the SBA-15 surface is 10.6%. This reflects the efficiency of alkyne derivatives of 1,3,5-triazine to react with azido-functionalized mesoporous silica through Huisgen's 1,3-cycloaddition resulting in triazole linkages.

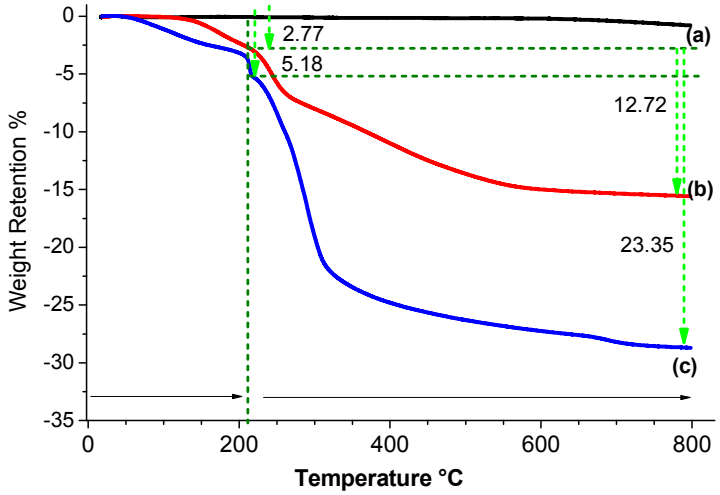

Figure 5 Thermogravimetric analysis of pristine mesoporous silica SBA-15 (a), N_3-SBA-15 (b), and 3Tr-M-SBA-15 (c).

3.1.5. Textural studies.

High-resolution transmission electron microscopy (HR-TEM) has been used in order to visually detect the presence of palladium nanoparticles, their dispersion and to verify their size distribution. The TEM image of the SBA-15 sample (Figure 6a) exhibits large domains of highly ordered stripe-like arranged structures, which accounts for the 2D hexagonal arrangement of uniformely sized 1D channels.

TEM images Figure 6(b,c,d) of the front and side views of the nanocatalyst show that palladium has been introduced within the channels of the structure. This suggests that the mesoporous silica possesses sufficient structural stability required to retain morphological integrity despite the loading of metal NPs. Black dots, observed in the TEM images of the resulting nanocomposite materials, are assigned to Pd(0) NPs.[52] Indeed, after the anchoring of Pd(II) complex inside the mesoporous channels of SBA-15, the image displays distinct deep

contrasting meso parallel channels with respect to the light shaded surface (Figure 6b).[53] This might be interpreted as due to the presence of the 3Tr-M–Pd complex mostly inside the mesopores of the SBA-15, yet some nanoparticles are loaded on the surface of the hybrid support.

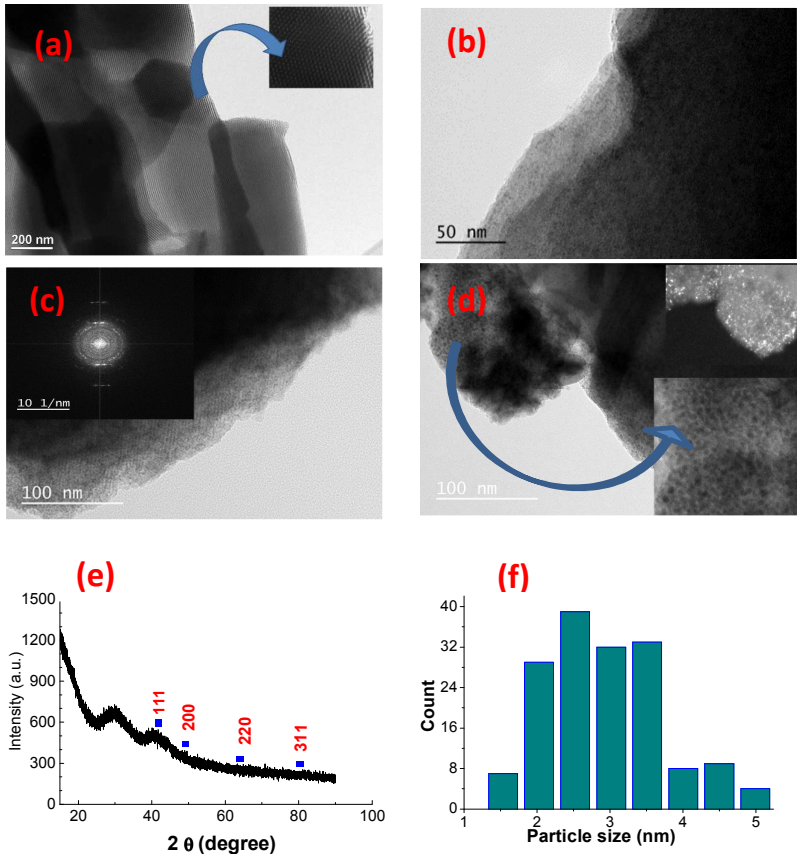

Figure 6. (a) Typical TEM images of SBA-15 (a), and Pd(0)/3Tr-M-SBA-15 nanocatalyst (b,c,d). XRD pattern of nanocatalyst (e) and histogram of the Pd particle size distribution (f).

The catalyst Pd(0)/3Tr-M-SBA-15 is characterized by XRD, and their XRD patterns are shown in Figure 6e. Three peaks at 2θ of 40.0°, 48.1° and 66.4° corresponding to the diffraction of the (1 1 1), (2 0 0) and (2 2 0) lattice planes of the Pd nanoparticles planes in the face centered cubic (FCC) crystal structure of Pd [54] and the broad peak centred at 2θ of 23° corresponding to the support of the mesoporous silica can be clearly observed.

The histogram in Figure 6e exhibits a narrow size distribution of the Pd nanoparticles with a mean value of 3.154 ±0.49 nm indicating that palladium nanoparticles did not aggregate upon immobilization. Indeed, the formation of small palladium particles is ascribed to the use of the reducing agent $NaBH_4$ which permits their quick nucleation and growth.[38]

3.1. Catalytic performance

Nitrophenol (4-NP) is a water pollutant with high toxicity, which is of great environmental concern.[55] Its reduced form 4-aminophenol is an important analogue of anilines, an intermediate of several antipyretic and analgesic drugs such as paracetamol and acetanilide. Hence, many processes have been developed for the NP removal such as adsorption, microbial degradation, photocatalytic degradation of p-nitrophenol (p-NP) into p-aminophenol (p-AP) by catalytic hydrogenation and stoichiometric reduction. In this regard, metal NPs can be active catalysts for several electron-transfer reactions. In this study, we evaluated the catalytic activity of the Pd(0)/3Tr-M-SBA-15 in the model reaction of reduction of p-nitrophenol to p-aminophenol with an excess amount of $NaBH_4$.

The reduction process was monitored using UV−vis spectroscopy at different time intervals (Figure 7c). In the absence of any Pd(0)/3Tr-M-SBA-15 the reduction reaction does not proceed even in a large excess of $NaBH_4$. Indeed, the absorption of 4-nitrophenol in water gives a characteristic peak at 317 nm which is simply shifted to 400 nm after addition of $NaBH_4$ without any significant decrease in peak intensity. This change from light to dark yellow resulting in spectral shift to 400 nm (Figure 7a) is due to the formation of the corresponding nitrophenolate anion.

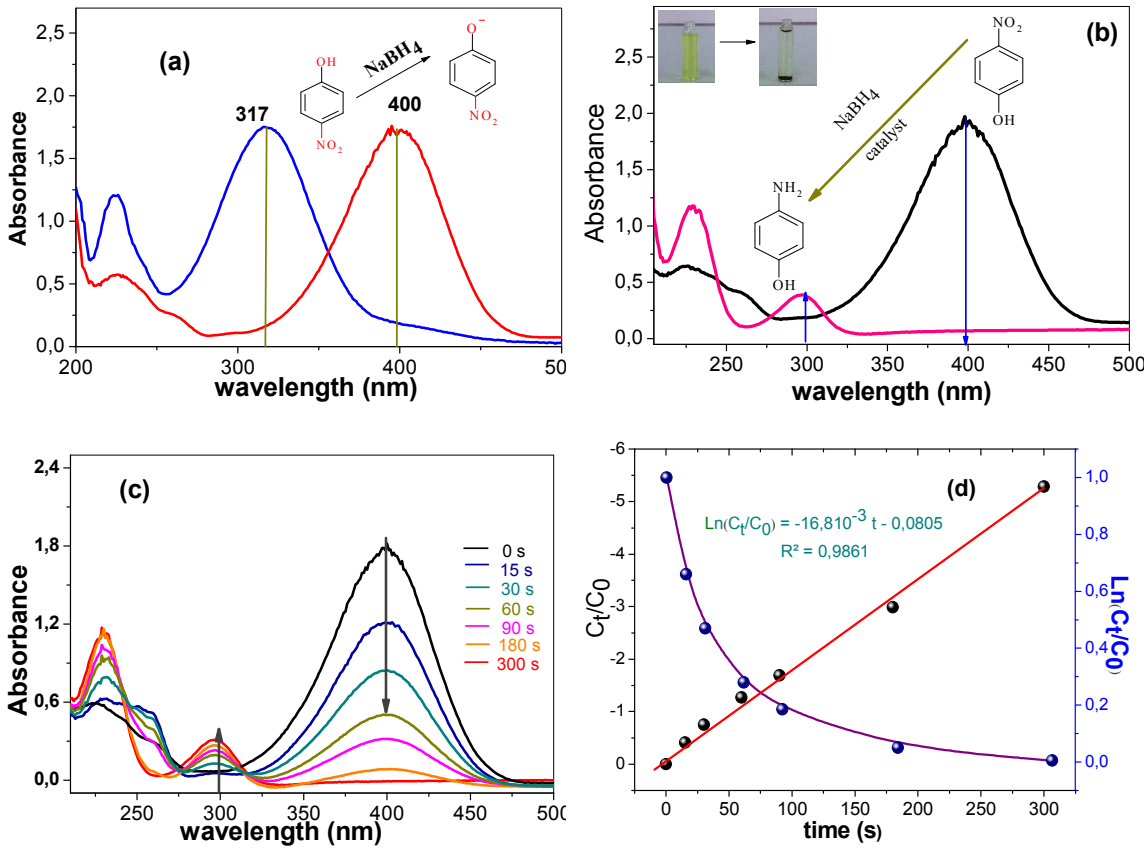

Figure 7. (a) UV-vis spectra of 4-nitrophenol before and after adding $NaBH_4$ solution, (b) Reaction scheme for the reduction of p-nitrophenol to p-aminophenol, (c) Time-dependent UV-vis spectral changes in 4-NP catalyzed by Pd(0)/3Tr-M-SBA-15 at 25 °C, (d) Linear relationship of $\ln(C_t/C_0)$ as a function of time.

The reduction of the nitro-group does not take place in the absence of any catalyst due to a high kinetic barrier between the mutually repelling negative ions, 4-NP and BH_4^-.[56] In the presence of SBA-15, the concentration of p-nitrophenol decreased marginally (5-7 %), due to adsorption on the surface. In contrast, when Pd(0)/3Tr-M-SBA-15 nanocatalysts were introduced into the solution, the absorption band of the p-nitrophenolate ion at about 400 nm gradually decrease and the color of the solution vanished thus indicating the reductive transformation of 4-nitrophenol into 4-aminophenol (Figure 7b). The bright yellow solution gradually turns colorless 600 s after adding the catalyst, a visual inspection that supports the complete reduction of 4-nitrophenol. The formation of 4-aminophenol was confirmed by the appearance of intense bands at 230 and 310 nm indicating that the $–NO_2$ group of p-nitrophenol has been reduced to the $–NH_2$ group.

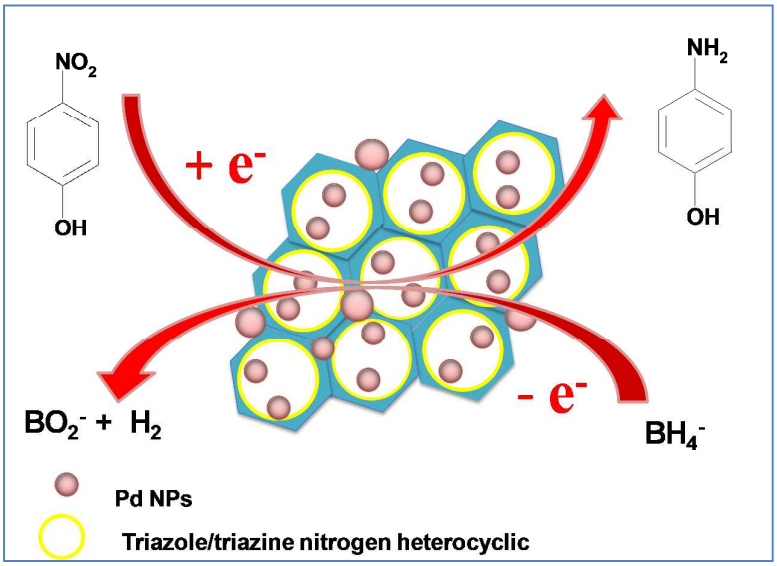

Figure 8. The proposed mechanism of the conversion of 4-NP to 4-AP by Pd(0)/3Tr-M-SBA-15.

On the basis of the catalytic reduction of 4-NP to 4-AP by Pd(0)/3Tr-M-SBA-15 schematized in Figure 8, the catalytic mechanism of the reduction reaction can be described as follows: both the donor BH_4^- ions and the acceptor 4-NP molecules adsorb onto the catalytic centers with a result of electron transfer from the former to the latter. This process leads to the reduction of 4-NP into 4-aminophenol.

The efficiency of the catalytic conversion of p-nitrophenol (4-NP) into p-aminophenol (4-AP) can be calculated using equation (1):

$$(4-NP)\% = \frac{(C_0 - C_t)}{C_0} X\ 100 \qquad (1)$$

where C_t is the concentration of 4-NP measured at time t, and C_0 is the initial concentration of 4-NP at time zero.

The reaction kinetics can be described by equation (2):

$$\frac{d[4-NP]}{dt} = k_{app}[4-NP]^n \qquad (2)$$

where k_{app} is the apparent rate constant and n is the reaction order of [4-NP].

In this study, $NaBH_4$ was used in excess, and the catalytic reduction is assumed to be a pseudo-first-order process. The $\ln(C_t/C_0)$-vs-time plot is obtained by monitoring the absorbance as a function of time (equation 3):

$$-k_{app}t = \ln(\frac{C_t}{C_0}) \quad (3)$$

where C_t and C_0 are defined as above, and k_{app} is the kinetic constant. Figure 7d exhibits an excellent linear fit for the reduction reaction catalyzed by Pd(0)/3Tr-M-SBA-15. By monitoring the decrease in the absorption band of the enolate ion at 400 nm, and assuming pseudo-first order kinetics, it was possible to determine an apparent rate constant (see Figure 7c). The whole reaction is almost complete within 300 s in the presence of excess $NaBH_4$. For the Pd(0)/3Tr-M-SBA-15 catalyst the kinetic rate constant (ka_{pp}) at RT equals to 16.8×10^{-3} s^{-1} and is comparable to previously published data for other supports.[56,57]

The high catalytic activity might be attributed to the structure of the hybrid platform for nano palladium catalyst and the very small Pd nanoparticles on the substrate.

Pd(0)/3Tr-M-SBA-15 catalyst was prepared and served to catalyze conversion of 4-NP to 4-AP three times. After the first run, the catalyst was washed three times sequentially with ethanol, water and a solution of sodium carbonate (0.3 mol L^{-1}) in order to remove borates and any other reaction byproducts remaining from the previous run. The washed catalyst was then further used again to verify the stability of its catalytic performances.

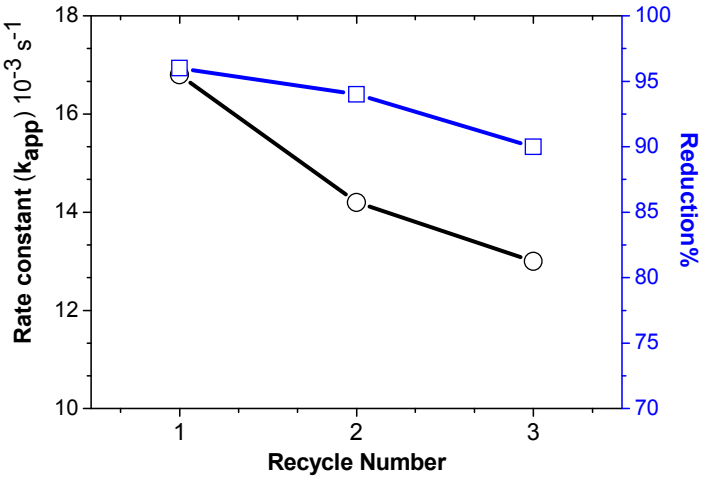

Figure 9. Recycling test of Pd(0)/3Tr-M-SBA-15 catalyst in water medium catalytic conversion of 4-NP to 4-AP.

Figure 9 displays the recycling test of Pd(0)/3Tr-M-SBA-15; a marginal decrease of the kinetic constant values k_{app} is noted. The k_{app} constant in the third cycle was found to be as high as 13.1 indicating that the catalyst exhibits a good stability against poisoning by the product of the reaction. The percentage of completion reduction (CR) was nearly the same in the first two cycles, decreasing only marginally (CR~90%), possibly due to the leaching of a small portion of Pd NPs from the hybrid support, to the oxidation of palladium upon exposure to air or to the screening of the catalytic sites by the formed product.[58] However, the latter hypothesis could be ruled out as the hybrid catalysts were thoroughly washed after each catalytic process.

4. Conclusions

In summary, novel 1,2,3-triazoles from alkyne derivatives of 1,3,5-triazines complex over the surface of organo-functionalized N_3-SBA-15 and subsequent complexation with palladium chloride have been fabricated by click reactions. The complexation of this ligand with $PdCl_2$ was performed to prepare heterogeneous catalytic systems. Modified SBA-15 and Pd(0)/3Tr-M-SBA-15 were analyzed by XPS, XRD, N_2 sorption measurement isotherm, TGA, FT-IR and TEM. XPS and FT-IR spectroscopy results are consistent with the covalent attachment of the heterocyclic organic moieties to the the surface of SBA-15 as well as inside the silica channels. TEM images showed that Pd NPs are remarkably well dispersed on the hybrid SBA-15 network the structure of which is hexagonal. The SBA-15 based catalysts have high surface area as judged by BET technique. The thermal stability of Pd(0)/3Tr-M-SBA-15 was monitored by TGA. The catalytic activity of newly synthesized heterogeneous catalyst was assessed in the reduction of p-nitrophenol the rate of which was found to be as high as 16.8×10^{-3} s^{-1}.

This work conclusively shows that the dual-functional click-generated triazole-triazine/SBA-15 system acts as a unique hybrid platform for the in situ synthesis and immobilization of palladium nanocatalysts. High surface concentration and robust attachment of the Pd NPs are due to the central role of the dendron-like structure provided by triazine and triazole heterocycles. These mini-dendrons act as strong anchoring sites for the catalyst nanoparticles. While the demonstration of proof of concept is provided herein with the catalyzed reduction

of p-nitrophenol, the ternary SBA-15/nitrogen heterocyle/Pd NP hybrid nanocatalyst has certainly much to offer and could be envisaged for the catalysis of other reactions. Last but not least, one can benefit from the strategy described above as the hybrid catalytic system can be obtained in high yield, which anticipates the scalability of our protocol.

Acknowledgements

AS is indebted to the Tunisian Ministry of Higher Education and Scientific Research for the provision of travel grants to conduct research at ICMPE. All authors thank Ms Sena Hamadi for her assistance with TGA analyses.

Supporting Information

The Supporting Information is available free of charge on the ACS Publications website.

Surface chemical composition of the hybrid nanocatalyst and the SBA-15 and N_3-SBA-15 precursors and solid state ^{13}C cross-polarized magic angle spinning (CP-MAS) NMR spectra of hybrid materials.

References

(1) Pozun, Z. D.; Rodenbusch, S. E.; Keller, E.; Tran, K.; Tang, W.; Stevenson, K. J.; Henkelman, G. A systematic investigation of p-nitrophenol reduction by bimetallic dendrimer encapsulated nanoparticles. *J. Phys. Chem. C* **2013**, *117*, 7598-7604.

(2) Morère, J.; Tenorio, M. J.; Torralvo, M. J.; Pando, C.; Renuncio, J. A. R.; Cabanas, A. Deposition of Pd into mesoporous silica SBA-15 using supercritical carbon dioxide. *J. Supercrit. Fluids.* **2011**, *56*, 213-222.

(3) Yan, R.; Xu. J; Zhang, Y.; Wang, D.; Zhang, M.; Zhang, W. Simultaneous Pd catalyst immobilization during synthesis of mesoporous silica. *Chem. Eng. J.* **2012**, *200–202*, 559–568.

(4) Ghorbani-Vaghei, R.; Hemmati, S.; Hashemi, M.; Veisi, H. Diethylenetriamine-functionalized single-walled carbon nanotubes (SWCNTs) to immobilization palladium as a novel recyclable heterogeneous nanocatalyst for the Suzuki–Miyaura coupling reaction in aqueous media. *C. R. Chimie*. **2015**, *18*, 636-643.

(5) Jawale, D. V.; Gravel, E.; Boudet, C.; Shah, N.; Geertsen, V.; Li, H.; Namboothiri, I. N. N.; Doris, E. Room temperature Suzuki coupling of aryl iodides, bromides, and chlorides

using a heterogeneous carbon nanotube-palladium nanohybrid catalyst. *Catal. Sci. Technol*. **2015***, 5*, 2388-2392.

(6) Havasi, F.; Ghorbani-Choghamarani, A; Nikpour, F. Pd-Grafted Functionalized Mesoporous MCM-41: A Novel, Green and heterogeneous nanocatalyst for the selective synthesis of phenols and anilines from aryl halides in water. *New J. Chem*. **2015**, *39*, 6504-6512.

(7) Opanasenko, M.; Štěpnička, P.; Čejka, J. Heterogeneous Pd catalysts supported on silica matrices, *RSC Adv*. **2014**, *4*, 65137–65162.

(8) Li, C.; Sato, T.; Yamauchi, Y. Size-controlled synthesis of mesoporous palladium nanoparticles as highly active and stable electrocatalysts. *Chem. Commun.* **2014**, *50*, 11753-11756.

(9) Li, C.; Jiang, B.; Miyamoto, N.; Kim, J. H.; Malgras, V.; Yamauchi, Y. Surfactant-directed synthesis of mesoporous Pd films with perpendicular mesochannels as efficient electrocatalysts. *J. Am. Chem. Soc.* **2015**, 137, 11558-11561.

(10) Malgras, V.; Ataee-Esfahani, H.; Wang, H.; Jiang, B.; Li, C.; Wu, K. C.-W.; Kim, J. H.; Yamauchi, Y. Nanoarchitectures for mesoporous metals. *Adv. Mater*., **2016**, *28*, 993-1010.

(11) Bernini, R.; Cacchi, S.; Fabrizi, G.; Forte, G; Petrucci, F; Prastaro, A.; Niembro, S.; Shafir, A.; Vallribera, A. Perfluoro-tagged, phosphine-free palladium nanoparticles supported on silica gel: application to alkynylation of aryl halides, Suzuki–Miyaura cross-coupling, and Heck reactions under aerobic condition, *Green Chem*. **2010**, *12* ,150–158.

(12) Lu, X.; Bian, X.; Nie, G.; Zhang, C.; Wang, C.; Wei, Y. Encapsulating conducting polypyrrole into electrospun TiO_2 nanofibers: a new kind of nanoreactor for in situ loading Pd nanocatalysts towards p-nitrophenol hydrogenation. *J. Mater. Chem*. **2012**, *22*, 12723-12730.

(13) Gu, X.; Qi, W.; Xu, X.; Sun, Z.; Zhang, L.; Liu, W.; Pan, X.; Su, D. Covalently functionalized carbon nanotube supported Pd nanoparticles for catalytic reduction of 4-nitrophenol. *Nanoscale.* **2014**, *6*, 6609-6616.

(14) Le, X.; Dong, Z.; Liu, Y.; Jin, Z.; Huy, T.-D.; Le, M.; Ma, J. Palladium nanoparticles immobilized on core–shell magnetic fibers as a highly efficient and recyclable heterogeneous catalyst for the reduction of 4-nitrophenol and Suzuki coupling reactions. *J. Mater. Chem. A.* **2014**, *2*, 19696-19706.

(15) Huang, J.; Yin, J.; Chai, W.; Liang, C.; Shen, J.; Zhang, F. Multifunctional mesoporous silica supported palladium nanoparticles as efficient and reusable catalyst for water-medium Ullmann reaction, *New J. Chem*. **2012**, *36*, 1378–1384.

(16) Zhang, F.; Yang, H. Multifunctional mesoporous silica-supported palladium nanoparticles for selective phenol hydrogenation in the aqueous phase. *Catal. Sci. Technol*. **2015**, *5*, 572-577.

(17) Saad, A.; Snoussi, Y.; Abderrabba, M.; Chehimi, M. M. Ligand-modified mesoporous silica SBA-15/silver hybrids for the catalyzed reduction of methylene blue. *RSC Adv*. **2016**, *6*, 57672-57682.

(18) Chang, W. C.; Deka, J. R.; Wu, H. Y.; Shieh, F. K.; Huang, S. Y.; Kao, H. M. Synthesis and characterization of large pore cubic mesoporous silicas functionalized with high contents of carboxylic acid groups and their use as adsorbents. *Appl. Catal. B*. **2013**, *142–143*, 817–827.

(19) Huang, Z; Che, S. Fabrication of mesostructured silica materials through co-structure-directing route. *Bull. Chem. Soc. Jpn*. **2015**, *88*, 617-632.

(20)Yamamoto, E.; Kuroda, K. Colloidal mesoporous silica nanoparticles. *Bull. Chem. Soc. Jpn.* **2016**, *89*, 501-539.

(21) Lian, H.-Y.; Liang, Y.-H.; Yamauchi, Y; Wu, K. C.-W. A hierarchical study on load/release kinetics of guest molecules into/from mesoporous silica thin films. *J. Phys. Chem. C*. **2011**, *115*, 6581-6590.

(22) Shieh, F. K; Hsiao, C. T; Kao, H.-M.; Sue, Y.-C.; Lin, K.-W.; Wu, C.-C.; Chen, X.-H.; Wan, L.; Hsu, M.-H.; Hwu, J. R.; Tsung, C.-K.; Wu, K. C.-W. Size-adjustable annular ring-functionalized mesoporous silica as effective and selective adsorbents for heavy metal ions. *RSC Adv*. **2013**, *3*, 25686–25689.

(23) Turgis, R.; Arrachart, G.; Delchet, C.; Rey, C.; Barré, Y.; Pellet-Rostaing, S.; Guari, Y.; Larionova, J.; Grandjean, A. An original "click and bind" approach for immobilizing copper hexacyanoferrate nanoparticles on mesoporous silica. *Chem. Mater.* **2013***, 25*, 4447-4453.

(24) Saad, A.; Abderrabba, M.; Chehimi, M. M. X-ray induced degradation of surface bound azido groups during XPS analysis. *Surf. Interface Anal*. **2017**, *49*, 340-344.

(25) De Los Cobos, O.; Fousseret, B.; Lejeune, M; Rossignol, F.; Dutreilh-Colas, M.; Carrion, C; Boissière, C. ; Ribot, F. ; Sanchez, C. ; Cattoën, X. ; Wong Chi Man, M.; Durand, J.-O. Tunable multifunctional mesoporous silica microdots arrays by combination of inkjet printing, EISA, and click chemistry. *Chem. Mater*. **2012**, *24*, 4337-4342.

(26) Gao, J.; Chen, J.; Li, X.; Wang, M.; Zhang, X.; Tan, F.; Xu, S.; Liu, J. Azide-functionalized hollow silica nanospheres for removal of antibiotics*, J. Colloid Interface Sci.* **2015**, *444*, 38-41.

(27) Malvi, B.; Sarkar, B. R.; Pati, D.; Mathew, R., Ajithkumar, T. G.; Gupta, S. S. "Clickable" SBA-15 mesoporous materials: synthesis, characterization and their reaction with alkynes. *J. Mater. Chem.* **2009**, *19*, 1409-1416.

(28) Nakazawa, J.; Smith, B. J.; Stack, T. D. P. Discrete complexes immobilized onto click-SBA-15 silica: controllable loadings and the impact of surface coverage on catalysis. *J. Am. Chem. Soc*. **2012**, *134*, 2750−2759.

(29) Kantheti, S.; Narayan, R.; Raju, K. V. S. N. The impact of 1,2,3-triazoles in the design of functional coatings. *RSC Adv*. **2015**, *5* , 3687-3708

(30) Ziarani, G. M.; Hassanzadeh, Z.; Gholamzadeh, P.; Asadi, S.; Badiei, A. Advances in click chemistry for silica-based material construction. *RSC Adv.* **2016**, *6*, 21979-22006.

(31) Huang, D.; Yang, G.; Feng, X.; Lai, X.; Zhao, P. Triazole-stabilized gold and related noble metal nanoparticles for 4-nitrophenol reduction. *New J. Chem.* **2015**, *39*, 4685-4694

(32) Basinska, T.; Slomkowski, S. Design of polyglycidol-containing microspheres for biomedical applications. *Chem. Pap.* **2012**, *66*, 352-368.

(33) Liu, J.; Zong, E.; Fu, H.; Zheng, S.; Xu, Z.; Zhu, D. Adsorption of aromatic compounds on porous covalent triazine-based framework. *J. Colloid Interface Sci.* **2012**, *372*, 99-107.

(34) Sang, J.; Aisawa, S.; Hirahara, H.; Kudo, T.; Mori, K. Self-reduction and size controlled synthesis of silver nanoparticles on carbon nanospheres by grafting triazine-based molecular layer for conductivity improvement. *Appl. Surf. Sci.* **2016**, *364*, 110-116.

(35) Sharma, P.; Singh, A. P. Synthesis of a recyclable and efficient Pd (II) 4-(2-pyridyl)-1,2,3-triazole complex over a solid periodic mesoporous organosilica support by "click reactions" for the Stille coupling reaction. *RSC Adv.* **2014**, *4*, 43070-43079.

(36) Chassaing, S.; Bénéteau, V.; Pale, P. When CuAAC 'Click Chemistry' goes heterogeneous. *Catal. Sci. Technol.* **2016**, *6*, 923-957.

(37) Zhao, D.; Feng, J.; Huo, Q.; Melosh, N.; Fredrickson, G. H.; Chmelka, B. F.; Stucky, G. D. Triblock copolymer syntheses of mesoporous silica with periodic 50 to 300 Angstrom pores. *Science.***1998**, *279*, 548-552.

(38) Chergui, S. M.; Ledebt, A.; Mammeri, F.; Herbst, F.; Carbonnier, B.; Ben Romdhane, H.; Chehimi, M. M. Hairy carbon nanotube@ nano-pd heterostructures: design, characterization, and application in Suzuki C−C coupling reaction. *Langmuir*. **2010**, *26*, 16115-16121.

(39) Brunauer, S., Emmett, P. H.; Teller, E. Adsorption of gases in multimolecular layers. *J. Am. Chem. Soc*. **1938**, *60*, 309-319.

(40) Barrett, E. P.; Joyner, L. G.; Halenda, P. P. The determination of pore volume and area distributions in porous substances. I. Computations from nitrogen isotherms. *J. Am. Chem. Soc.* **1951**, *73*, 373-380.

(41) Isfahani, A. L.; Mohammadpoor-Baltork, I.; Mirkhani, V.; Khosropour, A. R.; Moghadam, M.; Tangestaninejad, S.; Kia, R. Palladium nanoparticles immobilized on nano-silica triazine dendritic polymer (Pdnp-nSTDP): an efficient and reusable catalyst for Suzuki–Miyaura Cross-Coupling and Heck Reactions. *Adv. Synth. Catal.* **2013**, *355*, 957–972.

(42) Brunauer, S.; Deming, L. S.; Deming, W. E.; Teller, E. On a theory of the van der Waals adsorption of gases. *J. Am. Chem.Soc*. **1940**, *62*, 1723-1732.

(43) Hou, Y.; Ji, X.; Liu, G.; Tang, J.; Zheng, J.; Liu, Y.; Zhang, W.; Jia, M. Immobilization of palladium in N-heterocyclic carbene functionalized SBA-15 for the catalytic application in aerobic oxidation of benzyl alcohol. *Catal. Commun.* **2009**, *10*, 1459-1462.

(44) Castle J. E.; Watts, J. F. in Corrosion Control by Organic Coatings, ed. H. Leidheiser, NACE, Houston. **1981**, p. 78.

(45) Santos, C. M.; Kumar, A.; Zhang, W.; Cai, C. Functionalization of fluorous thin films via "click" chemistry. *Chem. Commun*. **2009**, 2854-2856.

(46) Zorn, G.; Liu, L.-H.; Árnadóttir, L.; Wang, H.; Gamble, L. J.; Castner, D. G.; Yan, M. X-ray photoelectron spectroscopy investigation of the nitrogen species in photoactive perfluorophenylazide-modified surfaces. *J. Phys. Chem. C* **2014**,*118*, 376-383.

(47) Powell, C. J. Recommended Auger parameters for 42 elemental solids. *J. Electron Spectrosc. Relat. Phenom*. **2012**, *185*, 1-3.

(48) Dhara, K.; Sarkar, K.; Srimani, D.; Saha, S. K.; Chattopadhyay, P.; Bhaumik, A. A new functionalized mesoporous matrix supported Pd (II)-Schiff base complex: an efficient catalyst for the Suzuki–Miyaura coupling reaction. *Dalton Trans.* **2010**, *39*, 6395-6402.

(49) Yang, H.; Han, X.; Li, G.; Wang, Y. N-Heterocyclic carbene palladium complex supported on ionic liquid-modified SBA-16: an efficient and highly recyclable catalyst for the Suzuki and Heck reactions. *Green Chem.* **2009**, *11*, 1184-1193.

(50) Veisi, H.; Hamelian, M.; Hemmati, S. Palladium anchored to SBA-15 functionalized with melamine-pyridine groups as a novel and efficient heterogeneous nanocatalyst for Suzuki–Miyaura coupling reactions *J. Mol. Catal. A Chem.* **2014**, *395*, 25-33.

(51) Gao, J.; Zhang, X.; Xu, S.; Tan, F.; Li, X.; Zhang, Y.; Qu, Z.; Quan, X.; Liu, J. Clickable periodic mesoporous organosilicas: synthesis, click reactions, and adsorption of antibiotics. *Chem. Eur. J.* **2014**, *20*, 1957-1963.

(52) Borah, P.; Zhao, Y. β-Diketimine appended periodic mesoporous organosilica as a scaffold for immobilization of palladium acetate: An efficient green catalyst for Wacker type reaction. *J. Catal.* **2014**, *318*, 43-52.

(53) Shephard, D. S.; Zhou, V.; Maschmeyer, T.; Matters, J. M.; Roper, C. L.; Parsons, S.; Johnson, B. F. G.; Duer, M. J. Site-directed surface derivatization of MCM-41: Use of high-resolution transmission electron microscopy and molecular recognition for determining the position of functionality within mesoporous materials. *Angew. Chem., Int. Ed.*, **1998**, *37*, 2719-2723.

(54) Jiang, H.; Yu, X.; Nie, R.; Lu, X.; Zhou, D.; Xia, Q. Selective hydrogenation of aromatic carboxylic acids over basic N-doped mesoporous carbon supported palladium catalysts. *Appl. Catal. A. General* **2016**, *520*, 73–81.

(55) Wu, K.-L.; Wei, X.-W.; Zhou, X.-M.; Wu, D.-H.; Liu, X.-W.; Ye, Y.; Wang, Q, $NiCo_2$ alloys: controllable synthesis, magnetic properties, and catalytic applications in reduction of 4-nitrophenol. *J. Phys. Chem. C.* **2011**, *115*, 16268-16274.

(56) Dong, Z.; Le, X.; Liu, Y.; Dong, C.; Ma, J. Metal organic framework derived magnetic porous carbon composite supported gold and palladium nanoparticles as highly efficient and recyclable catalysts for reduction of 4-nitrophenol and hydrodechlorination of 4-chlorophenol. *J. Mater. Chem. A*. **2014**, *2*, 18775-18785.

(57) Wang, Q.; Jia, W.; Liu, B.; Dong, A.; Gong, X.; Li, C.; Jing, P.; Li, Y.; Xy, G.; Zhang, J. Hierarchical structure based on Pd (Au) nanoparticles grafted onto magnetite cores and double layered shells: enhanced activity for catalytic applications. *J. Mater. Chem. A.* **2013,** *41*, 12732-12741.

(58) Muthuchamy, N.; Gopalan, A.; Lee, K.-P. A new facile strategy for higher loading of silver nanoparticles onto silica for efficient catalytic reduction of 4-nitrophenol. *RSC Adv.* **2015**, *5*, 76170- 76181.

ToC GRAPHIC

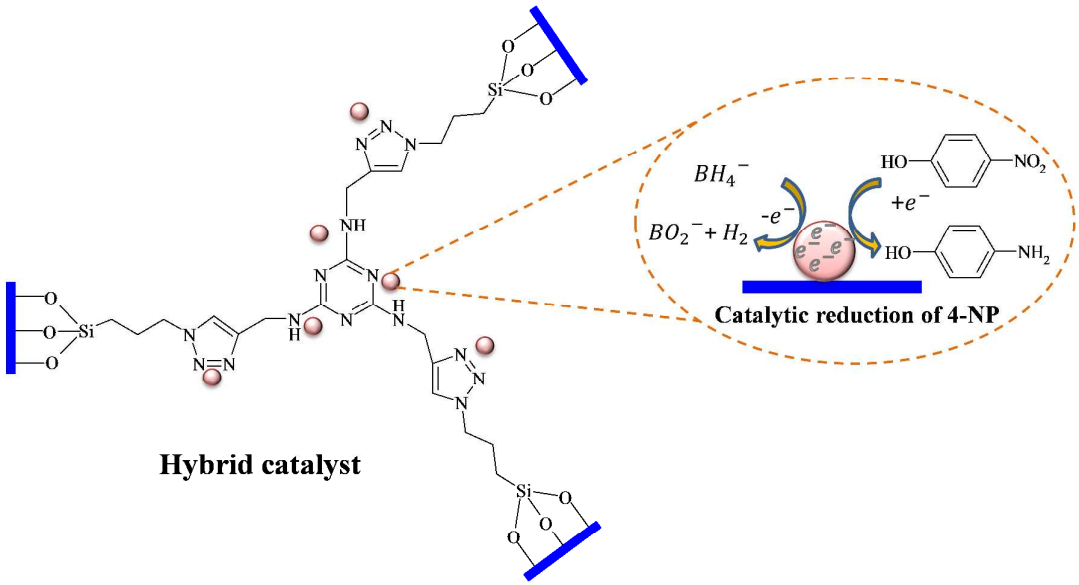
Hybrid catalyst
BH_4^-
$BO_2^- + H_2$
$-e^-$
$+e^-$
HO
NO_2
HO
NH_2
Catalytic reduction of 4-NP